A multi-mode driven high-performance color-changing window for building environmental protection

Lin Zhang*

Jiamusi University, Jiamusi, Heilongjiang, China

Abstract: In this study, an innovative smart window color-changing is assembled by cathode (Mo^WO_3) and anode (TiO_2). The color change performance of the window is improved by Mo doping (reversibility increased from 79.1% to 93.6%), and the color change effect of the window can be automatically adjusted by external illumination by TiO_2 on the anode. The microstructure and electrochromic behavior were characterized of the cathode. The microstructure was characterized of the anode. At the same time, the feasibility of discoloration of the device under light control is verified.

1 Introduction

The widespread global energy crisis and environmental deterioration, it is crucial to advance energy-efficient and carbon-neutral buildings [1]. With the continuous acceleration of urbanization, it also increases the energy needed to adjust the temperature of modern buildings [2,3]. Electrochromic (EC) smart windows can modulate sunlight irradiation entering a building by a low external voltage, which provides a feasible idea for reducing the energy consumption of the building [4-6]. Currently, the EC device mainly preparing a WO_3 film onto FTO or ITO coated glass, achieving optical modulation through the reversible redox reactions of WO_3 [7]. However, the dense microstructure of WO^3 thin films impedes the exchange of Li ions, significantly reducing the electrochromic performance [8]. Meanwhile, the EC device needs electric drive to complete color change, which seriously limits its application scope [9].

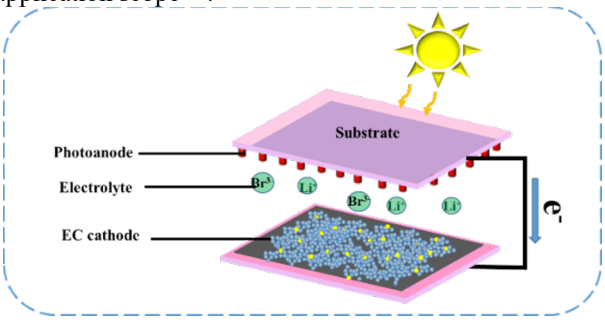

Fig. 1. Schematic diagram of multi-mode driving smart window

Fig. 1 shows the idea of this work. In the presence of an external electric field, a reversible redox reaction occurred in the thin film of the cathode: W^{6+}(bleached) is oxidized to W^{5+}(colored), Li ions are also embedded into the film surface from the electrolyte. When the photoanode is illuminated, the photosensitive dye at the anode excites the electrons, electrons are transported to the cathode film through external lines, so that it can complete the same redox reaction as that under electric control. The intensity of illumination is positively correlated with the number of electrons produced by photoanode. Therefore, the coloring and bleaching of the smart window can be realized under the electric control or the light control.

2 Results and discussion

In this work, Mo^WO_3 films were prepared by using Na_2WO_4 and Na_2MoO_4, adjusting the PH value of the mixed solution with HCl and $H_2C_2O_4$, and carrying out hydrothermal reaction in a constant temperature box at 170 ℃ for 1.1 h.

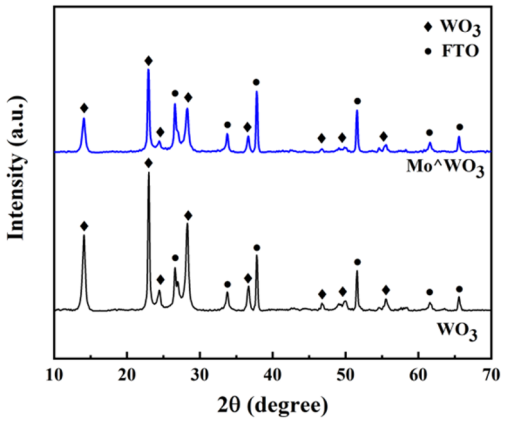

Fig. 2. XRD diffraction of the cathode

In order to explore the elemental composition of cathode film. The XRD diffraction of the sample is shown in Fig. 2. The characteristic peak of WO_3 can be observed in XRD (JCPDS no. 75-2187) [10]. However, the characteristic peak of Mo was not observed in XRD. This may be because the content of Mo is too low, and Mo

*e-mail: sudadaqiang@163.com

atoms may be doped in the lattice of WO_3, which leads to the inability of XRD instruments to detect the existence of Mo elements [11].

In order to prove the existence of Mo in the sample, the EDS diagram is shown in Fig. 3. The characteristic peaks of O, Na and W were observed in WO_3 samples, on the other hand, the characteristic peaks of O, Na, W and Mo were observed in Mo^WO_3 samples. Therefore, according to Fig 1. and Fig 2, it can be concluded that the WO_3 and Mo^WO_3 sample was successfully prepared.

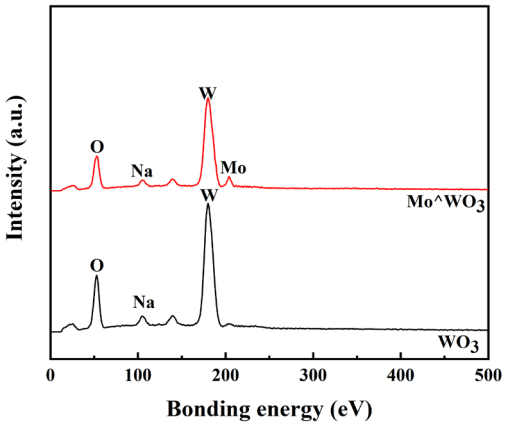

Fig. 3. EDS diagram of the cathode

To explore the morphological change after doping, Fig. 4 shows the SEM of WO_3 (Fig 4. (a)) and Mo^WO_3 (Fig 4. (b)) film. It can be seen that the surface of WO_3 sample presents a dense spherical micro-morphology. Due to the doping of Mo, the surface of Mo^WO_3 sample changed from dense structure to long granular and porous structure. Due to the porous surface of the doped structure, the ability of Li ions to be embedded/extracted in the color change reaction may be improved.

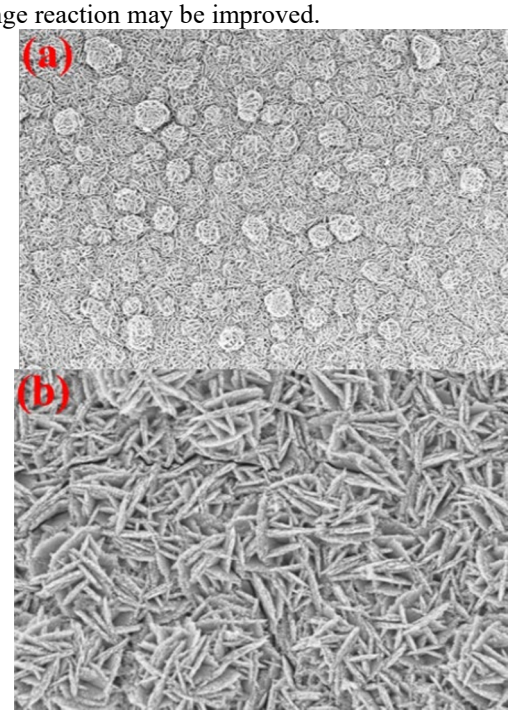

Fig. 4. SEM of WO_3 and Mo^WO_3 film

In order to determine the EC performance. The cyclic voltammetry was shown in Fig. 5. Fig. 5 shows that the closed curve area of Mo^WO_3 sample is larger than that of WO_3 sample. At the same time, the oxidation peak value of Mo sample is also higher than that of WO_3 sample. This strongly proves that the porous micro-morphology promotes the mobility of ions and electrons and improves the performance of EC.

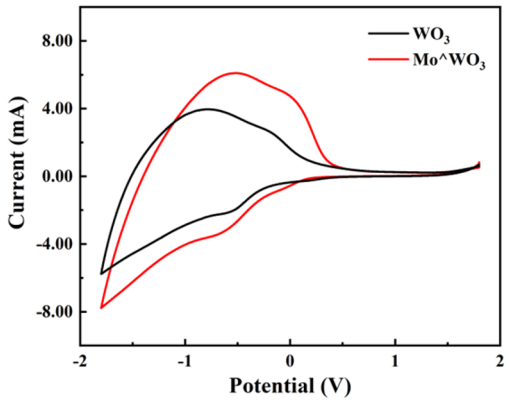

Fig. 5. Cyclic voltammetry of the cathode

In order to further explore the performance of doped EC. Fig. 6 shows the chronocoulometry curves of two samples. The reversibility of the sample can be obtained by positive/negative bias for 50 seconds, as shown in eq. 1:

$$\text{Reversibility} = \frac{Q_{di}\,(\text{Extracted charge})}{Q_i\,(\text{Injected charge})} \qquad (1)$$

Where Q_{di} is the charge extracted after direct voltage is applied. Q_i, Q_{di} is the insertion charge after negative voltage is applied. The reversibility of WO_3 and Mo^WO_3 samples obtained by eq. 1 are 79.1% and 93.6%, respectively. It is proved that the doping of Mo improves the electrochromic speed of the sample.

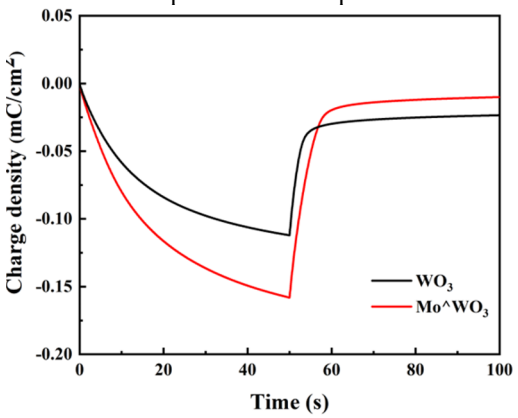

Fig. 6. Chronocoulometry of the cathode

In order to verify that Mo doping improves the transfer of electrons and the diffusion rate of Li ions. Fig. 7 shows the Nyquist curves. The curve consists of two parts, one of which is a semi-circular curve. The smaller the radius of the semicircle curve, the smaller the charge transfer resistance of the sample. The second part is a similar-line. The greater the slope of the diagonal line, the greater the diffusion rate of ions in the electrolyte. Therefore, Nyquist curves proves that the Mo^WO_3 sample has smaller charge

transfer resistance and larger ion diffusion rate. It is also proved that Mo doping improves the electrochromic properties of the samples.

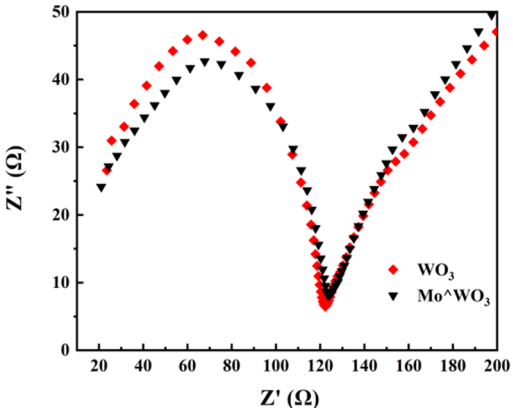

Fig. 7. Nyquist curves of the cathode

From Fig. 5, Fig. 6 and Fig. 7. It can be concluded that the doping of Mo provides porous structures on the surface of the film, which also enhances the ion exchange properties. Meanwhile, the coloration of WO_3 is realized by reversible chemical reaction. Therefore, the doping of Mo will improve the EC properties of the films.

To realize the light-driven mode, TiO_2 anode was prepared by hydrothermal method with $C_{16}H_{36}O4Ti$ and HCl as raw materials. The TiO_2 film was soaked in C_2H_6O with N719 for 48 hours.

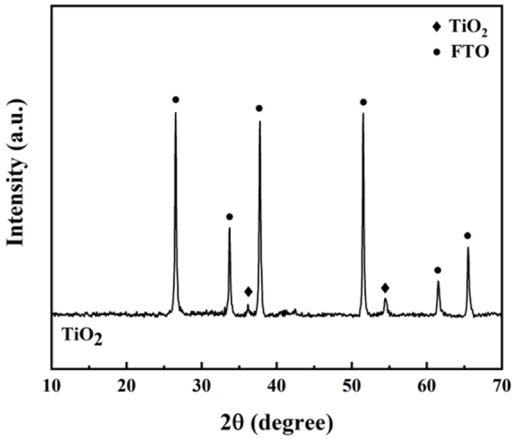

Fig. 8. EDS diagram of the anode

In order to explore the elemental composition of cathode film. The XRD diffraction of the sample is shown in Fig. 8. The characteristic peak of TiO_2 can be observed in XRD (JCPDS no. 73-1232) [12].

The EDS of the sample is shown in Fig. 9. The characteristic peaks of Ti, O, Sn and Ti were observed in samples. Therefore, according to Fig 7. and Fig 8, it can be concluded that the TiO_2 sample was successfully prepared.

To explore the morphological of anode. Fig. 10 shows the SEM of TiO_2 film. It can be seen that the surface of TiO_2 sample presents an inverted nanowire structure. This structure provides a lot of space for the attachment of photosensitive dyes. Photosensitive dyes have greater absorption ability to visible light, which further enhances the conversion ability of TiO_2 to light.

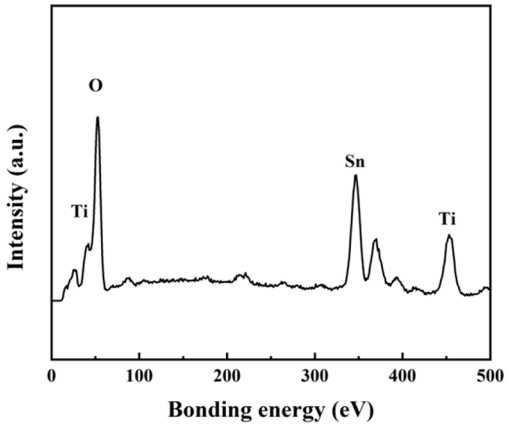

Fig. 9. EDS diagram of the anode

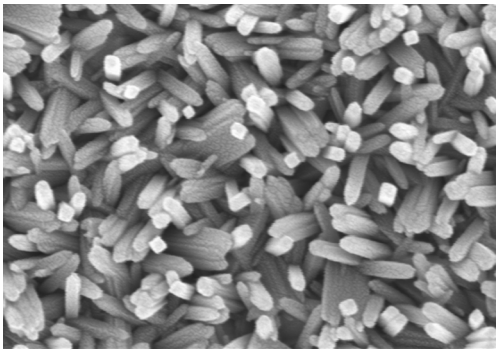

Fig. 10. SEM diagram of the anode

In order to prove the photoelectric conversion ability of the anode, the sample was irradiated by xenon lamp for 20 seconds, and the photocurrent was generated in different states of radiation and darkness. The transient photocurrent curve of the sample is shown in Fig. 11. From fig. 11, it can be found that under the illumination (20 to 40s), the generated photocurrent jumps from 0 to about 0.4 mA/cm^2, and then falls back to about 0.1 mA/cm^2 to be stable.

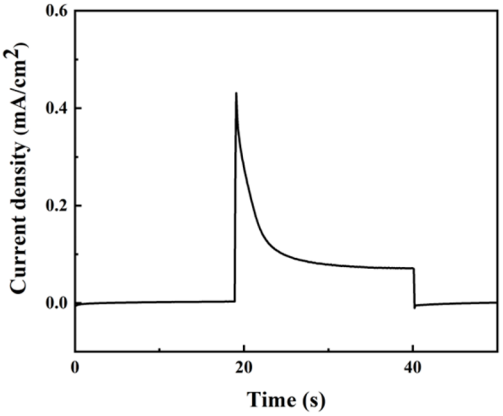

Fig. 11. Transient photocurrent curve

In order to verify the correctness of the assumption in this work. A device was fabricated by using TiO_2 and Mo^WO_3 film as cathode and anode respectively, placing

PTFE gasket in the middle and filling electrolyte of $LiClO_4$ and $C_{16}H_{36}BrN$.

Fig. 12 shows the color-changing effect of the assembled multi-drive high-performance color-changing window under illumination and apply electric field. The feasibility of electric drive and optical drive is proved. This proves that the smart window can adjust the transmittance of the device by the amount of charge, regardless of the electrical control. Under the light control, the intensity of light can be controlled to control the device. This device also verified that photogenerated electrons can provide power for electrochromic redox reaction.

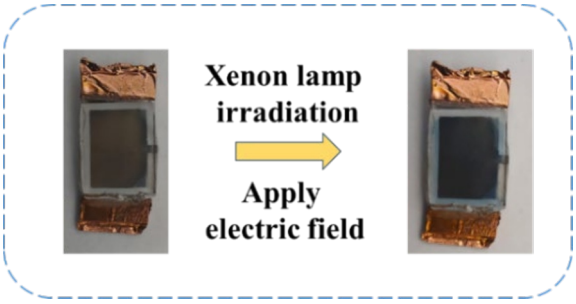

Fig. 12. Color-changing performance test of the device

3 Conclusion

In this paper, a multi-drive color-changing device composed of Mo^WO_3 and TiO_2 thin films was successfully fabricated. At the same time, it was proved that Mo doping changed the morphology of dense WO_3. The porous structure improves the transmission rate of electrons and the diffusion efficiency of ions. The electrochromic properties of the thin films were improved. On the other hand, nanowire TiO_2 was successfully prepared, which can improve the adhesion of photosensitive dyes and may improve the photoelectric conversion efficiency of electrodes. The anode and cathode are combined together, and electrolyte is filled in the middle to form a new intelligent window, which verifies the color-changing function of the device under light control and electric control. This work provides a new idea for environmental protection and energy saving of modern buildings.

Reference

1. Zhou Y. Artificial neural network-based smart aerogel glazing in low-energy buildings: A state-of-the-art review[J]. Iscience, 2021, 24(12).
2. Yang Q, Xiong J, Mao G, et al. A Novel Molecular PCM Wall with Inorganic Composite: Dynamic Thermal Analysis and Optimization in Charge–Discharge Cycles[J]. Materials, 2023, 16(17): 5955.
3. Ni X, Wu Z, Zhang W, et al. Energy utilization of building insulation waste expanded polystyrene: pyrolysis kinetic estimation by a new comprehensive method[J]. Polymers, 2020, 12(8): 1744.
4. Xie X, Ji H, Wang L, et al. Design and implementation of electrochromic smart windows with self-driven thermoelectric power generation[J]. Nanomaterials, 2024, 14(12): 1027.
5. Ke Y, Chen J, Lin G, et al. Smart windows: electro-, thermo-, mechano-, photochromics, and beyond[J]. Advanced Energy Materials, 2019, 9(39): 1902066.
6. Liu Y, Wang J, Wang F, et al. Full-frame and high-contrast smart windows from halide-exchanged perovskites[J]. Nature communications, 2021, 12(1): 3360.
7. Morankar P J, Amate R U, Bhosale M K, et al. PVP-Engineered WO_3/TiO_2 Heterostructures for High-Performance Electrochromic Applications with Enhanced Optical Modulation and Stability[J]. Polymers, 2025, 17(12): 1683.
8. Louloudakis D, Mouratis K, Gil-Rostra J, et al. Electrochromic response and porous structure of WO_3 cathode layers[J]. Electrochimica Acta, 2021, 376: 138049.
9. Gu C, Jia A B, Zhang Y M, et al. Emerging electrochromic materials and devices for future displays[J]. Chemical Reviews, 2022, 122(18): 14679-14721.
10. Sengupta S, Sudakar C, Kundu M. 3D-engineered WO3 microspheres assembled by 2D nanosheets with superior sodium storage capacity[J]. RSC advances, 2024, 14(22): 15706-15712.
11. Hong S, Yu F, Guo B, et al. Optimized fabrication of a Y-doped Ti/TiO2 macroporous membrane electrode and its application in the electrosynthesis of succinic acid[J]. RSC advances, 2025, 15(26): 21156-21167.
12. Chen Y, Liu B, Chen J, et al. Structure design and photocatalytic properties of one-dimensional SnO2-TiO2 composites[J]. Nanoscale Research Letters, 2015, 10(1): 200.